1GHz millivoltmeter

Rectifier-input instrument for use between 1kHz and 1GHz in the range 2mV-2V

N. G. MICHAELIDES

Broadband voltmeters can be distinguished into the following groups:

- meters with rectifier input
- meters with amplifier input
- meters employing sampling techniques

As for all voltage measuring meters, a high input impedance is essential.

METERS WITH RECTIFIER INPUT

In the simplest case, a detector probe is used in conjunction with a high-impedance electronic d.c. voltmeter. A high-frequency detector located in the probe head is employed to obtain a d.c. output proportional to the measured r.f. Detectors use high-frequency diodes in half-wave (Fig.1(a), (b)) or voltage/doubler (Fig.1(c)) rectifier circuits. For voltages over 1V, diode rectifiers function as peak amplitude detectors in which d.c. output is equal to the peak value minus the forward bias voltage of the diode. For voltages higher than 3V, diode bias can be neglected and the d.c. output of the detector, scaled down by 1.41 or 2.82, serves as a measure of the r.m.s. value of a pure sinusoid. Readings can be taken on the linear scale of the d.c. meter. For voltages lower than 3V, diode bias becomes significant and special non-linear scales are needed. Calibration is accurate for sinusoids.

The voltage range of this combination is from 0.1-0.3V to 10-20V. The upper limit is imposed by the reverse voltage rating of the diode and can it be extended with a divider. The lower limit is imposed by measurement accuracy. Below 100mV, accuracy degradation renders the meter useless. Accuracy is affected by compression of the non-linear scale at low voltages; different volt-ampere characteristics among diodes, requiring a one to one meter-probe calibration; and temperature dependence of the diode volt/ampere characteristic.

Millivolt ranges are characterized by the change in detector behaviour. Peak response gradually gives way to 'square-law' detection, which results in a non-linear detector response. To overcome this problem, along with the temperature dependence, some instruments use thermostatically controlled probes and linearizing electronic circuits.

Another approach, used in the present meter, is through a comparison detector. In this, two similar detector circuits are used: one rectifies the unknown r.f., while the other, a known, instrument-generated, comparison a.f. The amplitude of the comparison a.f. voltage is automatically controlled to give the same d.c. output as the r.f. one. It is evident that if the responses of the two detectors are close enough, so will be the magnitudes of the two signals. It is assumed here that the two detectors have a flat frequency response from a.f. to r.f. and are under the same thermal conditions: error can be introduced by diode mismatch and detector frequency response.

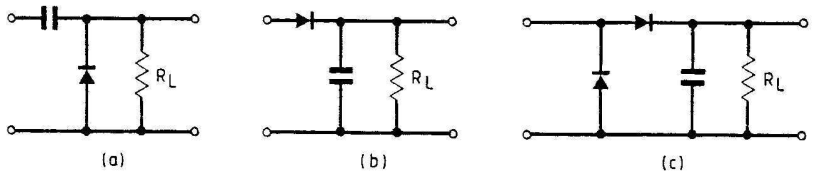

Fig.1. Forms of diode detector in half-wave (a,b) or full-wave (c) circuits.

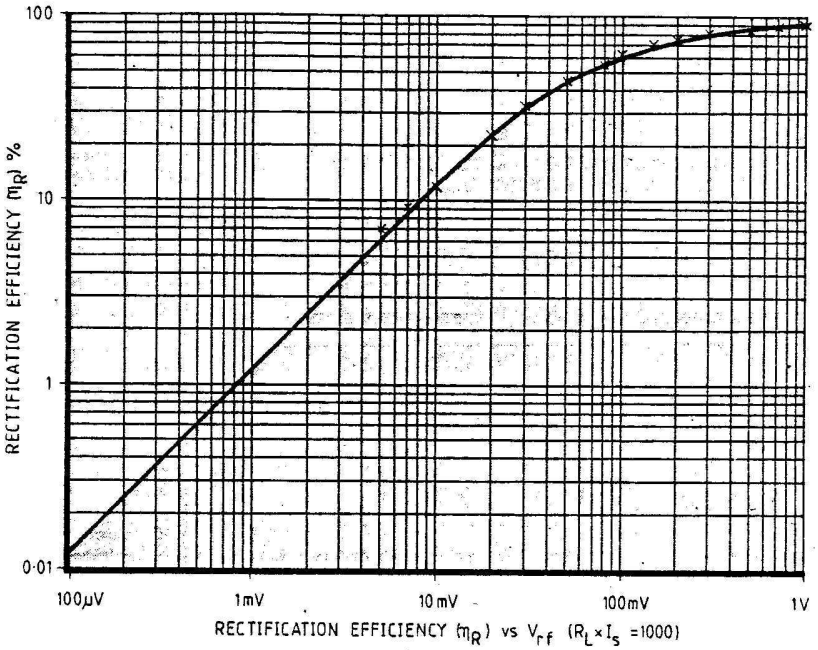

Fig.2. Computer plot of rectification efficiency of a half-wave circuit.

R.F. DETECTION

In a detection circuit (Fig.1) we can define for symmetrical waveforms the efficiency of rectification $n_R(v)$ as

$$\eta_R(v)=k\frac{V_{dc}}{V_{rfp}} \qquad (1)$$

where V_{dc} is the d.c. output of the detector,
V_{rfp} is the peak value of the detected r.f.,
k is a circuit factor, 1.0 for half-wave circuits and 0.5 for voltage-doubler circuits.

For sine waves $\eta_R(v)$ becomes

$$\eta_R(v)=k\frac{V_{dc}}{\sqrt{2}V_{rf}} \qquad (2)$$

where V_{rf} is the r.m.s. value of the detected r.f.

The output of a half-wave circuit (Fig.1(a), (b)) employing a diode that has a purely exponential characterisic defined by

$$I=I_S\left[\exp\left(\frac{V}{V_\tau}\right)-1\right] \qquad (3)$$

and provided that the internal resistance of the signal source is negligible, can be calculated[2] for the whole millivolt range from

$$I_0\left(\frac{\sqrt{2}V_{rf}}{V_\tau}\right)=\exp\left(\frac{V_{dc}}{V_\tau}\right)\left[1+\frac{V_{dc}}{R_L I_S}\right] \qquad (4)$$

where $I_0(x)$ is a modified Bessel function of the first kind and zero order,
V_T is the volt equivalent of temperature: for room temperature V_T=25.5mV,
I_s is the reverse saturation current of the diode,
R_L is the load resistance.

A computer plot of eq.(4) in the form $\eta_R(V_{rf})$ vs. V_{rf} is depicted in Fig.2. The Bessel integral.

$$I_0(x)=\frac{1}{2\pi}\int_0^{2\pi}\exp(x\cos\omega t)d\omega t \qquad (5)$$

was evaluated first using Simpson's rule for numeric integration. Then the two parts of eq.(4) were made equal by successive approximations. As can be seen, experimental results from a germanium diode detector are in excellent agreement with those theoretically predicted.

For small values of V_{rf}, the Bessel integral can be approximated by a series expansion

$$I_0(x)=1+\frac{x^2}{2^2}+\frac{x^4}{2^2 4^2}+\frac{x^6}{2^2 4^2 6^2}+\ldots \qquad (6)$$

Also exp(x) can be expanded

$$\exp(x)=1+x+\frac{x^2}{2!}+\frac{x^3}{3!}+\ldots \qquad (7)$$

Substituting the first two terms of the series expansions (6) and (7) and dropping V^2_{dc}, equation (4) becomes

$$V_{dc}=\frac{V^2_{rf}}{2V_\tau}\left[\frac{R_L I_S}{R_L I_S+V_\tau}\right] \qquad (8)$$

and for $R_L I_s \gg V_T$

$$V_{dc}=\frac{V^2_{rf}}{2V_\tau} \qquad (9)$$

V_{dc} calculated with eq. (8) has the following error over the exact solution of eq.(4):

+6.9% for V_{rf}=20mV
dropping to +2.0% for V_{rf}=10mV

Eq.(8), illustrated by the straight-line portion of the curve in Fig.2, indicates that for small V_{rf}, V_{dc} is proportional to the square of V_{rf}. For signals of V_{rf} = 30mV or less, the detector practically behaves as 'a square law' device. However, this square-law response offers both advantages and disadvantages.

The main advantage is that the detector has almost r.m.s. response regardless of the waveform of the measured signal. This is true only to a certain extent, depending on the voltage and the crest factor (ratio of peak to r.m.s.) of the waveform. Permissible crest factors for 2% and 5% error are given below:

V_{rf}	Crest factor
3mV	10/13
10mV	3/4
30mV	1.7/2

(source Rohde & Schwarz)

This property can be very useful in noise measurements. By insertion of a suitable attenuator or capacitive divider, higher voltages can be reduced to this level, thus extending upwards the almost true r.m.s. range.

On the other hand, the d.c. output of the detector falls/off rapidly with decreasing V_{rf}, becoming, below a certain value, unusable for further processing. For this reason, even the best professional meters have as their most sensitive subrange 3mV or 1mV f.s. To demonstrate this, a voltage-doubler detector will yield only 1.5 microvolt d.c. for 0.3mV r.f. In this low d.c. environment, the problems encountered are: noise (inherent and pick-up); thermocouple effects; short and long term thermal stability; electrostatically induced voltages; amplifier offsets; and printed-circuit leakage currents. The practice is to use a chopper-stabilized d.c. amplifier in the input stage. As an alternative a high-precision op-amp with comparable performance can be used.

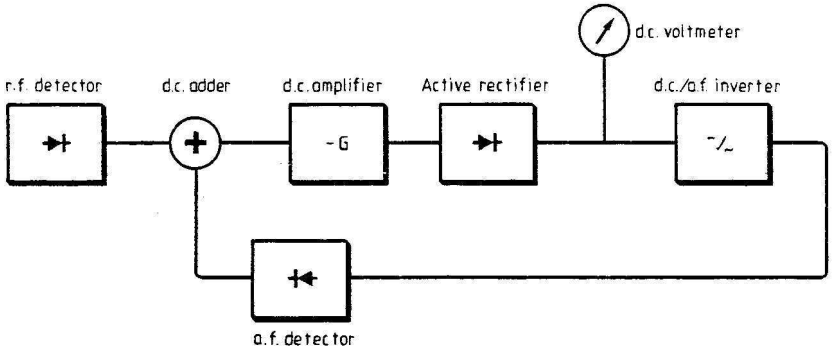

Fig.3. Block diagram of the millivoltmeter.

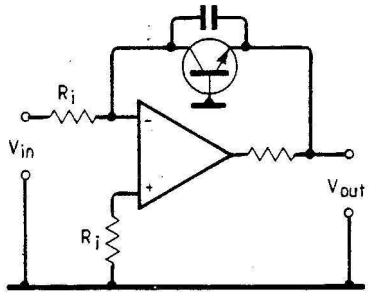

Fig.4. The use of log. amplifier obviates the need for elaborate switching. This is a basic circuit.

PRINCIPLE OF OPERATION

The principle of operation was used in a series of professional instruments manufactured by Rohde & Schwarz. During an attempt to re-design one such instrument[1], new circuits evolved that simplified circuitry astonishingly.

The r.f. to be measured and the comparison a.f. are rectified in the two similarly designed detector circuits (Fig.3, detectors 1,2) located in the probe head. The d.c. voltage difference of the two detector outputs is designated the error voltage

$$V_{err}=\frac{\sqrt{2}}{k}\left[\eta_R(V_{rf})V_{rf}-\eta_R(V_{af})V_{af}\right] \qquad (10)$$

The error voltage is then amplified by $-G$ and is ideally rectified, the rectified voltage being used for meter indication.

$$V_{ind}=G\,V_{err} \text{ for } V_{err}>0 \qquad (11)$$
$$V_{ind}=0 \quad \text{for } V_{err}<=0 \qquad (12)$$

The feedback loop closes with a d.c./a.f. inverter that generates a pure 5 kHz sine wave of V_{af} r.m.s. value, directly proportional to the absolute value of V_{ind}. Ratio of proportionally S is

$$S=\frac{V_{af}}{|V_{ind}|} \qquad (13)$$

Combining (10), (11), (13)

$$V_{ind}=\frac{G\eta_R(V_{rf})}{\frac{k}{\sqrt{2}}+GS\eta_R(S/V_{ind})}V_{rf} \qquad (14)$$

Examining eq.(14) one can see that it is a typical closed-loop transfer function of a control system. If $\eta_R(v)$ were constant, then the value of the fraction would have been constant and the relation between V_{ind} and V_{rf} linear throughout the meter range. The fraction contains $\eta_R(V_{rf})$ and $\eta_R(S/V_{ind})$ that are in general different by a small amount. In order to bring eq.(14) into common terms regarding $\eta_R(v)$ the following assumption is made:

$$\frac{\Delta\eta_R}{\Delta V}\approx\frac{d\eta_R(V_{rf})}{dV_{rf}} \qquad (15)$$

Eq.(15) is unconditionally true for V_{rf} <20mV (because $d\eta_R(V_{rf})/dV_{rf}$ is constant). For V_{rf}>20mV it is true for small ΔV. ΔV diminishes as G increases. Eq.(15) yields

$$\eta_R(S/V_{ind})=\eta_R(V_{rf})+a-a\frac{V_{rf}}{S/V_{ind}} \qquad (16)$$

where

$$a=\frac{d\eta_R(V_{rf})}{dV_{rf}}S/V_{ind} \qquad (17)$$

Rearranging, eq.(14) transforms to

$$V_{ind}=\frac{G[\eta_R(V_{rf})+a]}{\frac{k}{\sqrt{2}}+GS\left[\eta_R(V_{rf})+a\right]}V_{rf} \qquad (18)$$

The derivative $d\eta_R(V_{rf})/dV_{rf}$ in eq.(16) can be calculated analytically from

$$\frac{d\eta_R(V_{rf})}{dV_{rf}}=\frac{1}{\sqrt{2}V_{rf}}\left[\frac{dV_{dc}}{dV_{rf}}-\frac{V_{dc}}{V_{rf}}\right] \qquad (19)$$

$$\frac{dV_{dc}}{dV_{rf}}=\frac{\sqrt{2}I_1\left(\frac{\sqrt{2}V_{rf}}{V_\tau}\right)\left[R_L I_s+V_{dc}\right]}{I_0\left(\frac{\sqrt{2}V_{rf}}{V_\tau}\right)\left[R_L I_S+V_{dc}+V_\tau\right]} \qquad (20)$$

($I_1(x)$): is modified Bessel function of the first kind of first order.

A high degree of linearity can be achieved if $GS[\eta_R(V_{rf})+a] \gg k/\sqrt{2}$ throughout the

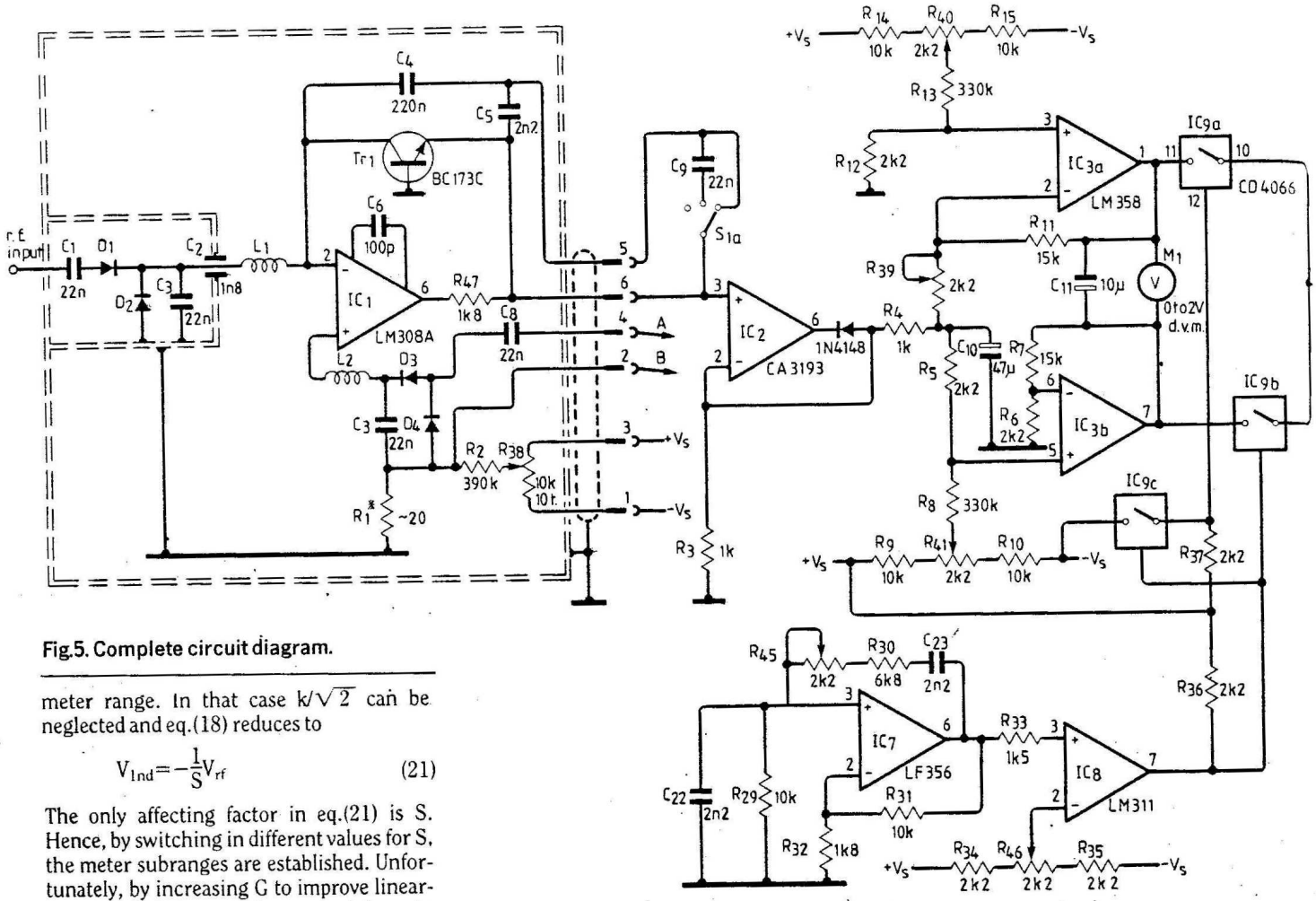

Fig.5. Complete circuit diagram.

meter range. In that case $k/\sqrt{2}$ can be neglected and eq.(18) reduces to

$$V_{1nd} = -\frac{1}{S}V_{rf} \qquad (21)$$

The only affecting factor in eq.(21) is S. Hence, by switching in different values for S, the meter subranges are established. Unfortunately, by increasing G to improve linearity, the tendency of the control loop to oscillate is increased. Stability can be maintained by giving G a frequency roll-off characteristic. For this reason, integrator capacitors are included in the d.c. path, but this prolongs response time.

A compromise between linearity, stability and response time can be reached. For this, in each subrange a suitable value for G is selected, such as to maintain $GS[\eta_R(V_e d2f)+a]$ within limits. The limits are determined by linearity imposing the lower limit ($GS[\eta_R(V_{rf})+a] \gg k/\sqrt{2}$), and control-loop stability imposing the upper limit. Hence, maximum G should be used for the minimum V_{rf} to be measured (where $[\eta_R(V_{rf})+a]$ and S are minimum) and vice-versas).

THE LOG. AMPLIFIER

The innovation of this design lies in the fact that the above goals are attained without the need for an elaborate switchable amplifier. Here a log. amplifier followed by a small-gain linear 'post amplifier' greatly simplify matters.

By this combination, as it will be shown, the dependence of V_{ind} on $[\eta_R(V_{rf})+a]$ is loosened and any desired degree of linearity between V_{ind} and V_{rf} can be achieved. A design requirement for 1:10 ratio subranges can thus be easily realised, in contrast with the switchable amplifier alternative.

Error voltage, eq.(10) modified by (15), (16), (17) becomes

$$V_{err} = \frac{\sqrt{2}}{k}\left[\eta_R(V_{rf})+a\right]\left[V_{rf} - S\cdot V_{ind}\right] \qquad (22)$$

Error voltage is applied in the input of the log. amplifier, (Fig.4) and its output, after being rectified (gain=1) and amplified by g is used as V_{ind}

$$V_{ind} = -gV_\tau \ln\left(\frac{V_{err}}{R_i I_t}+1\right) \qquad (23)$$

where R_i is the series input resistor,
I_t is the reverse saturation current of the transistor p-n junction,
g is the gain of the post amplifier.

Using the approximation $\exp(x) \sim (1+x)$, for small x and after some algebraic manipulation, V_{ind} takes the form

$$V_{ind} = -\frac{V_{rf}}{S} + \frac{\exp\left(\frac{V_{rf}}{SgV_\tau}\right)-1}{\exp\left(\frac{V_{rf}}{SgV_\tau}\right)\frac{1}{gV_\tau}+\frac{\sqrt{2}\,S[\eta_e(V_{rf})+a]}{kR_iI_t}} \qquad (24)$$

Eq.(24) is an improvement over eq.(18), since the expression containing $[\eta_R(V_{rf})+a]$ is no longer a multiplier of V_{rf} but a quantity to be subtracted, i.e. eq.(24) comprises two parts, a linear and a non-linear one. Also, $[\eta_R(V_{rf})+a]$ in the non-linear part is divided by an extremely small quanity, R_iI_t. the orders of magnitude of I_t and R_i are 10^{-14} A and 10^{+5} 214 respectively.

The magnitude of the non-linear factor, obviously affecting linearity, can be calculated by entering design values in eq.(24). The meter has three subranges: a) 2V-200mV, b) 200-20mV and c) 20-2mV. For compatibility with common d.v.ms, full-scale indication is 1.999V. Therefore, S values are: $S_a=1$, $S_b=0.1$ and $S_c=0.01$. In each subrange, the non-linear part has its highest value for the full-scale r.f. input. Among the three subranges maximum occurs for the 20mV r.f. input, where $[\eta_R(20mV)+a] = 0.47$ is lowest. It is interesting to note that the non-linear factor can be trimmed to any desired value, by proper g selection. A design value of $g=10$ was chosen, resulting in a linearity error of the order of 10^{-4}. Thus, method error is far below the one anticipated from other sources. For the accuracy sought, the non-linear factor can be neglected and eq.(24) reduces once again to eq.(21). On the other hand, excessive g is not favourable, as it affects stability by increasing the overall open-loop gain.

Summarizing, the log. amplifier functions as a self-controlled, high-gain amplifier. It exhibits the highest gain in the vicinity of zero input. Maximum gain is only limited by the open-loop gain of the op. amp. (typ. 300 000).This property of the log. amplifier is particularly useful in the microvolt range, where ample gain is essential. However, this is not the only affecting factor. Lowest-value measuring capability (sensitivity) is determined by zero stability and noise.

ZERO STABILITY

Zero offset (meter indication with no input) is unilateral, i.e. it is displayed only on the side of zero where the control loop is effective. In the other side, '00.00' is displayed regardless of offset. This, a consequence

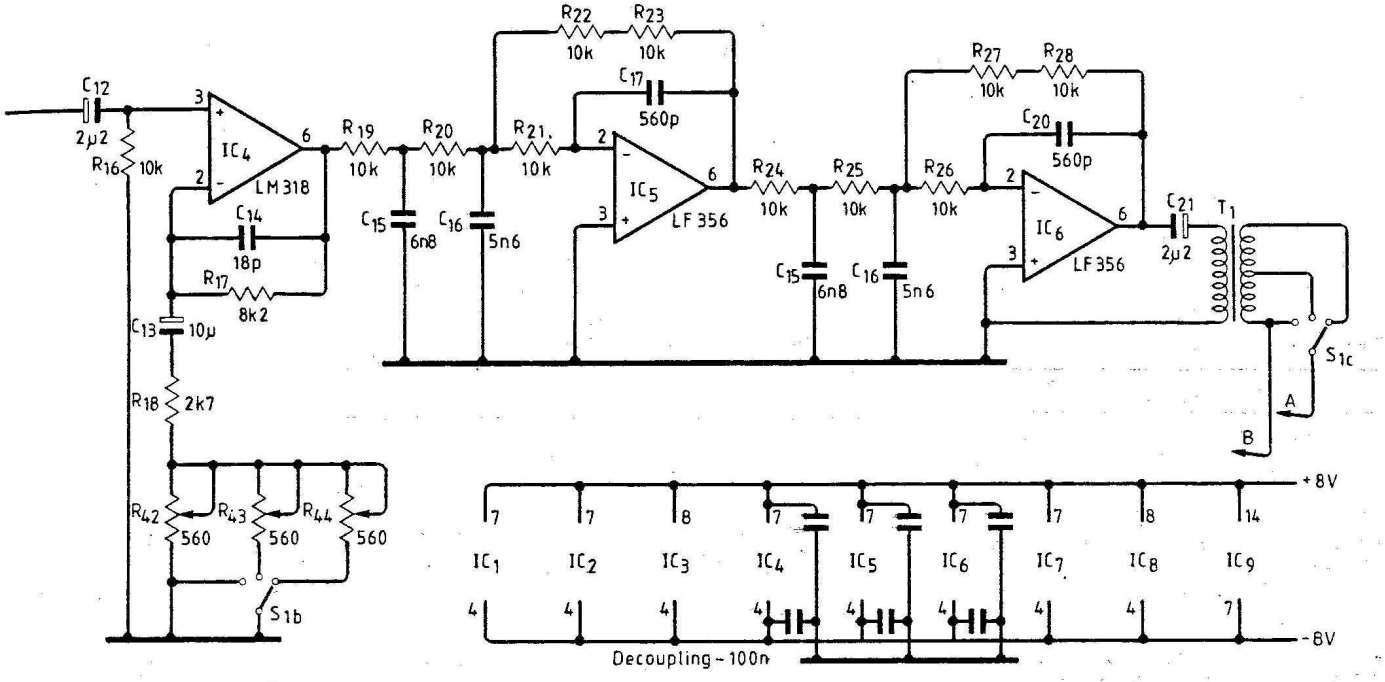

of the control function, can lead to erroneous measurements. It is therefore advisable to introduce deliberately an offset in the displayed side in order to avoid uncertainty.

If a zero offset exists (whether displayed or not), an input V_{rf} will be indicated as

$$V_{1nd} = -\frac{1}{S}\sqrt{v_{rf}^2 \pm V_{offs}^2} \qquad (25)$$

where V_{offs} is the displayed zero or an equivalent amount on the other side. The positive sign refers to the displayed offset while the negative to the non-displayed.

In the case of the displayed offset, eq.(25) indicates that: for V_{rf} much greater than V_{offs}, the error introduced by V_{offs} is negligible; for V_{rf} of the same order as V_{offs} the value of V_{rf} must be calculated from eq.(25); and for V_{rf} much smaller than V_{offs} the contribution of V_{rf} to V_{ind} is too small for accurate interpretation.

It is evidence that V_{offs} must be kept as low as possible. Moreover, the stability of V_{offs} with temperature and time is of great importance. The origin of V_{offs} lies in the existence of parasitic microvolt voltages within the sensitive part of the meter, namely the two detectors and the log. amplifier inputs – the most critical part of the meter. The rest is more or less straightforward.

CIRCUIT DESCRIPTION

The circuit diagram of the meter is depicted in Fig.5. Error voltage is first log. amplified (IC_1 in the probe), then rectified (IC_2) and low-pass filtered (R_4, C_{10}). The following stage ($IC_{3a,3b}$) is a balanced-to-ground, low output-impedance d.c. amplifier. Potentiometers R_{40}, R_{41} null offsets (zero meter indication with zero rectifier input), Balance is adjusted by means of R_{39} although metering is balance-error free. The output of the

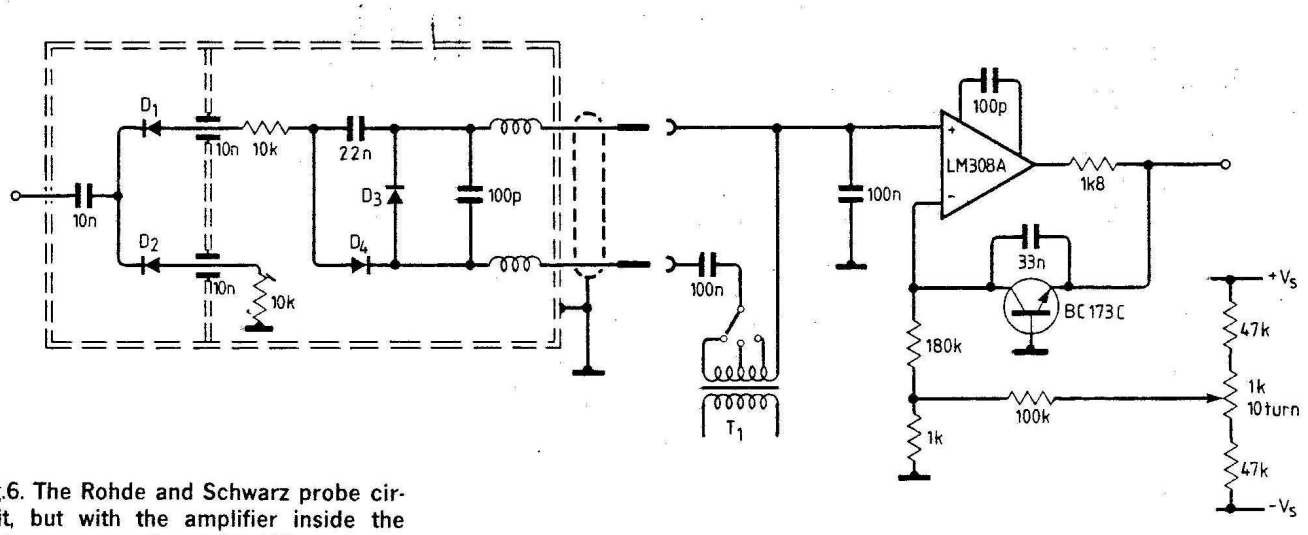

Fig.6. The Rohde and Schwarz probe circuit, but with the amplifier inside the meter, gave poor thermal stability.

succeeding chopper, a 5 kHz squarewave, is then amplified in meter calibration amplifier IC_4. This stage functions also as an impedance buffer between chopper and the first active filter. Separate calibration potentiometer, R_{42}, R_{43}, R_{44}, are provided for each subrange to compensate for minor discrepancies in transformer T_1 ratios. Two cascaded low-pass Butterworth active filters[3] (IC_5, IC_6) that follow, concert the squarewave into a sinusoidal voltage which, suitably divided by switchable ratio transformer T_1 (1:1, 10:1, 100:1), is finally delivered to the comparison detector in the probe. Auxiliary circuits to switch the chopper comprise, 5 kHz frequency oscillator IC_7, shaper-driver IC_8 and inverter-driver IC_{9c}. R_{45} and R_{46}.

THE PROBE CIRCUIT

The incorporation of the log. amplifier (IC_1, Tr_1) in the probe was dictated by the need to suppress thermocouple voltages. As a first approach the Rohde & Schwarz probe circuit was tried with the log. amplifier located in the meter body (Fig.6). The former, implemented with ordinary components, gave the meter poor zero thermal stability.

Zero thermal stability was enhanced by increasing circuit compactness by placing IC_1 close to the two detectors ($D_{1,2,3,4}$), and limiting the number of components to an absolute minimum. The use of carbon or metal-film resistors should be avoided (R_1 inevitably used in the nulling circuit is an r.f. choke functioning as a copper wire-wound resistor.) R_2 is not a part of the sensitive circuitry. The input circuit is guarded and IC_1, selected for low input-voltage offset, low offset drift and low noise.

The need for a screen between the two detectors degrades the probe stability during thermal transients, but elimination of the screen affects the frequency response of the probe. Diodes are socket-mounted (not soldered). Gold plated i.c. pin sockets are recommended. Integration capacitors $C_{4,5,9}$ are subrange selectable for best stability/response time performance. The zeroing adjustment R_{38} is incorporated in the probe to facilitate switching between probes without need for re-zeroing. The value of R_2 indicated in Fig.5 may need adjustment depending on R_1, IC_1 offset and diode matching.

DETECTOR DIODES

As already mentioned, meter accuracy and thermal stability greatly depend on the degree to which the four diodes ($D_{1,2,3,4}$) are matched. Ideally, all diodes should have identical volt/ampere characteristics within a wide temperature range.

Among many types of r.f. germanium diodes that were tested, in lots of 10 to 40 per type, no pair of exactly identical diodes was found. Discrepancies were noticed in their characteristics in both the forward and reverse bias state, as well as in their temperature dependence. Fortunately, a reasonable amount of mismatch can be tolerated before its effects become noticeable. Also, instead of four matched units, two matched pairs, each split between the two detectors, suffice.

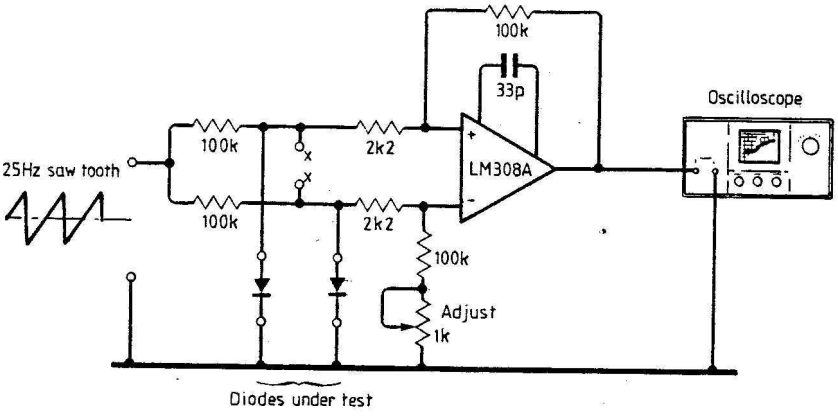

Fig.7. Circuit to assist diode pairing.

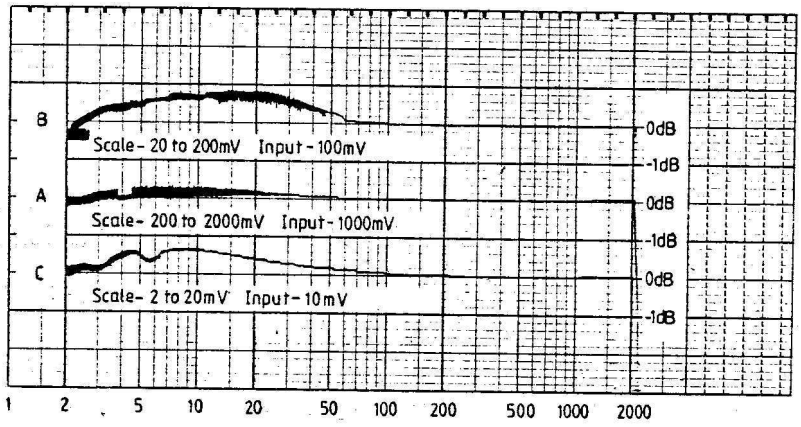

Audio frequency response of the instrument.

Inevitable residual mismatch also affects meter zero. Nulling is easily accomplished, along with op-amp offset, via R_{38}. Furthermore, the drift of the meter zero caused by temperature change of this residual mismatch can be benefically used to compensate inverse drift of the op-amp offset. Thus, by proper arrangement of the four diodes in the two detector circuits, thermal stability can be improved.

For diodes available in quantities, a preselection was made by sorting them according to their forward-bias voltage measured with a multimeter. Various groups having closely similar values were formed, and preference was given to the most numerous group having the lowest voltage value. Although the latter is not of much importance, it is nevertheless a welcome property, because it indicates a high I_s (refer to eq.(8)). Pairing was assisted by the tester of Fig.7, in which the degree of match between two diodes is better as the oscilloscope travel approaches a straight line. Best matches were tested (in the same way) in other ambient temperatures.

This procedure, being almost a d.c. test, is a measure of the performance of the diodes in the l.f. and h.f. spectrum. V.h.f. and u.h.f. efficiency evaluation was performed in the actual meter. Here again, discrepancies were noticed among previously matched diodes. Thermal stability and frequency response optimization was the criterion for the final selection and positioning of the pairs.

Diodes of the types AA112, AA113 and AA119 were tested in quantities, with satisfactory results. Any of these types can be used. A smaller number of OA90, OA95 and AAY11 was also tested. A limited number of 'gold-bonded' type (1N270 and 1N995) showed better temperature behaviour. Unfortunately, this cannot take the form of a general rule due to the small number tested and the unavailability of other types of this variety for cross-checking. Manufacturer's pairs were also not available for testing.

OTHER CONSIDERATIONS

Other factors that, in a lesser degree, affect meter accuracy are, firstly, error due to temperature de-calibration. Meter calibration assumes a stable relation between oscillator frequency and filter frequency response. Uneven temperature drift in the corresponding circuits (IC_5, IC_6, IC_7) alters this relation and thus, meter calibration becomes temperature sensitive. By using temperature-stable capacitors, properly matched, the 5 kHz frequency oscillator and the two active filters can be made to drift evenly. In this way, de-calibration error on the prototype was limited to <0.2% from 0 to 50°C.

Secondly, there is a linearity error due to distortion of the 5 kHz sinewave. The meter measures the d.c. value of the a.f. envelope. Detection of low voltages is r.m.s. sensitive. Any change in the relation between the envelope d.c. and the a.f. r.m.s. affects

linearity, mostly in the most sensitive subrange. Distortion, harmonics, line hum and modulation must be avoided. Measurements on the prototype showed <1% t.h.d. and harmonic levels <−47dB for the 2nd and <−50dB for the 3rd respectively. The transformer used is purpose wound on a ferrite core for low distortion. Primary and secondary have 2,000 turns, while the taps are on 200 and 20 turns. Transistor-radio audio transformers of suitable turns ratio can be used as an alternative. Modulation can occur from control-loop instability, but the specified capacitors $C_{4,5,9,10}$ ensure stable operation. The a.f. comparison voltage must be free from a.m. modulation with c.w. r.f. meter input. The r.m.s. value of a modulated signal is

$$V_{rms}=V_c\sqrt{1+\frac{m^2}{2}}$$

where V_c is the r.m.s. value of the carrier,
V_m is the r.m.s. value of the modulating signal
m is the degree of modulation V_m/V_c

PERFORMANCE

The meter was tested in conjunction with Rohde and Schwarz SMS-type r.f. signal generator. Linearity was tested throughout the meter range, at 10 MHz, with the generator terminated into 50 ohms. Composite generator-meter error (expressed as a percentage of the reading, not of the f.s. value) is

subrange	error
2V -200mV	+/−1.5%
200mV- 20mV	+/−0.7%
20mV - 2mV	+/−0.5%

The same results were obtained with the generator unterminated. For the frequency-response test, the generator was left unterminated in order to reduce to the minimum the components between generator and probe. One N-type-to-BNC adaptor was inevitably used. The frequency response of the generator-adaptor-probe combination for one of the prototype probes is given above.

Among the above voltage levels a frequency-response disagreement can be noticed. It can be readily explained by the variance of the input impedance with V_{rf}. Indicated approximate impedance values are for <10 MHz.

subrange	V_{rf}	input impedance	frequency 10mHz	100MHz	250MHz	500MHz	1GHz
2V −200mV	1V	100kΩ/4pF	0dB	−0.4dB	−0.5dB	+0.5dB	+1.7dB
200mV− 20mV	100mV	45kΩ/5pF	0dB	−0.3dB	−0.6dB	−0.7dB	−2.1dB
20mV − 2mV	10mV	20k6pF	0dB	−0.3dB	−0.7dB	−1.0dB	−3.1dB

Input capacitance given includes shunt capacitance of the diodes, stray capacitance and that of the BNC connector. More moderate values of the order 3 to 4pF are possible.

Sensitivity at 10 MHz is 0.2mV for one stable digit, 0.5mV for two stable digits and 1.0mV for three stable digits.

References

1. Rohde & Schwarz: 'URV RF-DC Millivoltmeter' (operation and service manual).
2. R. W. Landee, D. C. Davis, A. P. Albrecht, L. J. Giacolleto: 'Electronics designers' handbook', McGraw-Hill, New York, 1977, pp. 24-138, 24-142.
3. National Semiconductor: 'Audio handbook', 1976, pp. 5-3, 5-5.

Nicos Michaelides obtained his degree in electrical engineering, National Technical University of Athens, in 1973. He is currently working for the Greek Radio Television ERT.